Electronic structure and optical properties of Al and Mg co-doped GaN*

Ji Yan-Jun(纪延俊)[a], Du Yu-Jie(杜玉杰)[a]†, and Wang Mei-Shan(王美山)[b]

[a] *Department of Physical and Electronic Science, Bingzhou Univercity, Bingzhou* 256603, *China*
[b] *School of Physics and Optoelectronic Engineering, Ludong University, Yantai* 264025, *China*

(Received 4 March 2013; revised manuscript received 22 April 2013)

The electronic structure and optical properties of Al and Mg co-doped GaN are calculated from first principles using density function theory with the plane-wave ultrasoft pseudopotential method. The results show that the optimal form of p-type GaN is obtained with an appropriate Al:Mg co-doping ratio rather than with only Mg doping. Al doping weakens the interaction between Ga and N, resulting in the Ga 4s states moving to a high energy region and the system band gap widening. The optical properties of the co-doped system are calculated and compared with those of undoped GaN. The dielectric function of the co-doped system is anisotropic in the low energy region. The static refractive index and reflectivity increase, and absorption coefficient decreases. This provides the theoretical foundation for the design and application of Al–Mg co-doped GaN photoelectric materials.

Keywords: GaN, first-principles, electronic structure, optical properties

PACS: 71.55.Eq, 78.20.Ci **DOI:** 10.1088/1674-1056/22/11/117103

1. Introduction

GaN is a photoelectron material used in blue light-emitting diodes, blue lasers, and ultraviolet detectors.[1–6] It has promising applications in the field of electronic devices,[7–9] such as radioresistant, high-frequency, high-temperature, high-power, and optoelectronic devices. Pure GaN is an n-type conductive material.[10] Doping is an effective means of improving the photoelectric properties of materials, and the use of Mg as an effective p-type dopant was first reported by Akasaki *et al.*[11] The molecular structure, electronic properties, optical properties, and magnetic resonance characteristics of GaN and the polarity reversal of GaN surfaces after Mg doping were then investigated experimentally and theoretically.[12–16] The band gap widens and the emission wavelength spans from visible light to part of the ultraviolet region after GaN film has been doped with Al. The electronic structures and optical properties of $Al_xGa_{1-x}N$ heterojunctions grown on a GaAs substrate using molecular beam epitaxy have been studied by As *et al.*[17] The $Al_xGa_{1-x}N$ intermediate buffer layer with different doping concentrations was produced by Jang *et al.*[18] using the metalorganic vapour phase epitaxy method, and they found that the Al composition had a large influence on the crystal lattice. Li[19] theoretically studied Al-doped blende GaN compounds with different doping concentrations, and found that the lattice constant linearly decreased with the increase in doping concentration of Al. Lee *et al.*[20] obtained the hole concentration of Mg-doped $Al_xGa_{1-x}N$ experimentally. In the present paper, wurtzite GaN with different Mg–Al co-doping concentrations are calculated, and the optimum co-doping proportion with which the optimal form of GaN can be obtained is determined. The electronic structure and optical properties of the optimal co-doped GaN form are analyzed, and its mechanism is investigated.

2. Theoretical model and calculation method

The wurtzite GaN structure has *P*63*mc* symmetry. With the symmetry of C_{6v-4}, the lattice parameters can be described by $a = b = 0.3189$ nm, $c = 0.5185$ nm,[21] $\alpha = \beta = 90°$, and $\gamma = 120°$, where c/a is 1.626. All calculations are performed with the Cambridge Serial Total Energy Package (CASTEP). The Broyden–Fletcher–Goldfarb–Shanno (BFGS) algorithm is used to relax the structure of the crystal model. Exchange and correlation effects are treated with the generalized gradient approximation (GGA) implemented using the Perdew–Burke–Ernzerh (PBE) functional[22] and ultrasoft pseudopotentials.[23] Using periodic boundary conditions, the valence electronic wave functions are expanded in a plane wave basis set up to an energy cutoff of 400 eV. The interaction between the ion core and valence electrons is described by the ultrasoft pseudopotential method. The convergence accuracy is set to be a change in energy of less than 2×10^{-6} eV per atom, forces less than 0.005 eV/nm, the convergence tolerance of a single atomic energy below 1×10^{-5} eV per atom, the stress less than 0.05 GPa, and the change in displacement less than 0.0001 nm in the iterative process. The integral in the Brillouin zone is sampled with the Monkhorst–Pack

*Project supported by the National Natural Science Foundation of China (Grant No. 61171042), the Natural Science Foundation of Shandong Province, China (Grant No. ZR2010FL018), and the Doctoral Foundation of Binzhou University, China (Grant No.2012Y01).

†Corresponding author. E-mail: duyujie442@163.com

© 2013 Chinese Physical Society and IOP Publishing Ltd

scheme[24] and special k-points of high symmetry. The number of k points used is $9 \times 9 \times 9$ after a series of tests and consulting the literature,[25–27] which is sufficient for the convergence of the electronic and optical properties. All of the calculations are carried in reciprocal space with Ga: $3d^{10}4s^24p^1$, N: $2s^22p^3$, Al: $3s^2\ 3p^1$, and Mg: $2p^63s^2$ as the valence electrons.

3. Form of doped system

3.1. GaN compounds doped respectively with Mg and Al

In the calculations, $2 \times 2 \times 2$ supercells of wurtzite GaN are constructed. One Ga atom is replaced by a Mg or Al atom in the center of the supercells. The GaN supercells before and after doping with Mg(Al) are optimized, and the lattice parameters of GaN before and after Mg(Al) doping are shown in Table 1.

Table 1. Lattice parameters of GaN before and after Mg(Al) doping.

	GaN	GaN:Mg	GaN:Al
a	3.2248	3.2422	3.2113
b	3.2248	3.2422	3.2113
c	5.2535	5.2869	5.2264

It can be seen from Table 1 that the lattice parameters increase after Mg doping, while they decrease after Al doping. This is mainly due to the covalent bonds between N and Al atoms being stronger than those between N and Ga atoms, therefore, the lattice parameters decrease after Al doping. After Mg doping, the ionic bonds between N and Mg atoms are enhanced, and the lattice parameters increase. Therefore, co-doping should give a more stable crystal form.

3.2. GaN co-doped with Mg and Al

The lattice contraction coefficient is defined as[28]

$$\beta = -\frac{1}{a_0}\frac{\mathrm{d}a_0}{\mathrm{d}N_\mathrm{D}}, \tag{1}$$

where a_0 is the lattice constant, N_D is the doping concentration, and the effective lattice constant, $a_\mathrm{eff} = (\sqrt{3}a^2c)^{1/3}$, is used for a_0. The values of a_eff for GaN doped with Mg and Al are 0.0262 and -0.0206 compared with that of pure GaN, so the best co-doping proportion of Mg:Al is 1:1.27.

The volumes of the $2 \times 2 \times 2$-GaN supercells doped with different Mg and Al concentrations are shown in Table 2. With the increase in the Mg–Al doping concentration, the crystal volume gradually increases, and is close to the pure GaN supercell volume when the Mg:Al doping ratio is 1:1.27, i.e., it is almost the same when three Mg and four Al atoms take the place of seven Ga atoms. Thus, the optimum ratio of Al:Mg:Ga is 4:3:9 in the $2 \times 2 \times 2$-GaN supercell. GaN co-doped with Mg and other co-dopants has been studied experimentally and theoretically,[27,29,30] and the ratio of Al:Ga in experiment reached 7:3,[31] therefore, the above result is consistent with the experimental result.

Table 2. Values of volume, final energy, formation energy, and band gap for different compounds.

System	GaN	$Ga_{14}N$: Mg_1Al_1	$Ga_{12}N$: Mg_2Al_2	$Ga_{10}N$: Mg_3Al_3	Ga_9N: Mg_3Al_4	Ga_7N: Mg_4Al_5
Volume/nm^3	0.3785	0.37905	0.38005	0.38105	0.3785	0.38015
Final energy/eV	–37197.4	–34122.8	–31048.1	–27973.4	–25978.9	–22904.2
Formation energy/eV		–0.686	–1.294	–1.775	–3.627	–4.202
Bottom of the conduction band	1.664	2.004	2.304	2.496	2.654	2.907
Top of valence band	0	0.207	0.268	0.307	0.258	0.245
Energy gap/eV	1.664	1.797	2.036	2.189	2.395	2.662

The final energy is expressed by the Mermin finite temperature in CASTEP as

$$E = E_\mathrm{KS} - TS, \tag{2}$$

where E_KS is the Kohn–Sham energy, which ignores the entropy, T is the temperature, and S is the Mermin entropy due to the different ways in which the partially filled bands can be occupied.

The formation energy of the doped system is defined as

$$E_\mathrm{f}[X] = E_\mathrm{tot}[X] - E_\mathrm{tot}[\mathrm{GaN, bulk}] - \sum_i n_i\mu_i, \tag{3}$$

where $E_\mathrm{tot}[X]$ is the total energy of the GaN supercell doped with X, E_tot[GaN, bulk] is the total energy of the equivalent pure GaN supercell, n_i is the number of atoms of i, where $n_i > 0$ when atoms are added to the supercell and $n_i < 0$ when atoms are removed from the supercell, and μ_i is the chemical potential of atom i.

The formation and final energies of different doped systems are shown in Table 2. The formation energy decreases with doping concentration, which suggests that it is easier to dope as the doping concentration increases. The final energy increases with doping concentration increasing, which suggests that the doped system becomes increasing less thermodynamically stable as the doping concentration increases.

4. Electronic structure of the Mg–Al co-doped system

The band structures and density of states (DOS) of GaN before and after optimum Mg–Al co-doping are shown in Figs. 1–4. The dotted lines indicate the Fermi level. There is a deep acceptor level at –39.50 eV after Mg doping, but this

is not discussed here as it is so far away from the Fermi level. The DOS curve becomes smoother after Al–Mg co-doping by comparing Fig. 2 with Fig. 4, which means that the effective mass of carriers decreases and the nonlocality is enhanced. There is a direct transition band gap at the *G* point after doping at 2.39 eV (Fig. 3), and GaN retains a direct band gap semiconductor after Al–Mg co-doping. The DOS of the optimum Mg–Al co-doped GaN has contributions from N 2p, Ga 4s, and Ga 4p states, and slight contributions from Al 3s, Al 3p, N 2s, Mg 2p, and Mg 3s states in the lower electronic energy region (–7 eV–2 eV), while it mainly has contributions from the Ga 4s, Ga 4p, N 2p 2s, Al 3p, and Mg 2p states and slight contributions from Al 3s and Mg 2s states in the higher energy region (2 eV–5 eV). The top of the valence band is determined by the N 2p state electrons, while the bottom of the conduction band is determined by the Ga 4s state electrons. The band gap of co-doped GaN increases by 0.73 compared with that of pure GaN (1.66 eV, Fig. 1), this phenomenon is the same as that in Ref. [32]. The replacement of Ga by Al reduces the peak of the Ga partial DOS, the peak position changes, the bottom of the conduction band becomes smoother, and the Ga 4s states move to a higher energy, resulting in an increase in band gap. The system shows p-type conductive characteristics, mainly because of the excess carriers-holes at the top of valence band introduced by Mg doping. N 2p states move to a high energy for the hybridization of N 2p and Mg 2p states, so that the Fermi level moves into the valence band. The top of the valence band increases with doping concentration increasing when the same Mg:Al doping proportion is maintained, while it decreases with doping concentration increasing when the Al doping concentration is greater than the Mg concentration (see Table 2). This illustrates that the appropriate control of the Al doping concentration can overcome the repulsive interactions between acceptors produced by Mg doping only, and reduce the acceptor level. This is of significance in improving GaN p-type doping.

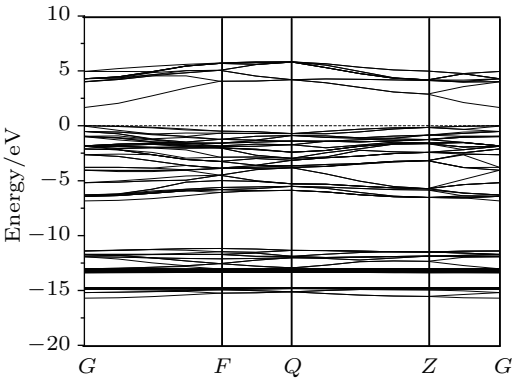


Fig. 1. Energy band structures of GaN.

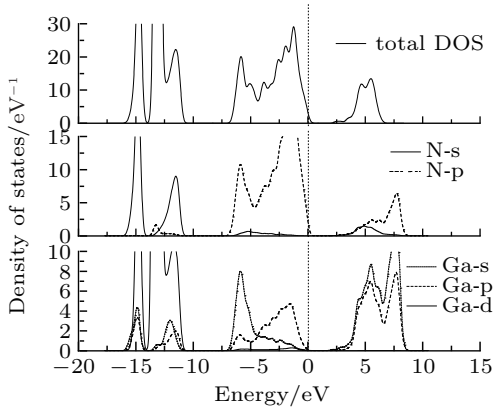


Fig. 2. Partial and total DOSs of GaN.

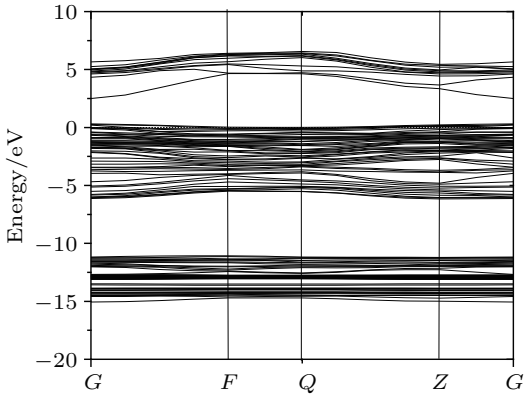


Fig. 3. Band structures of $Al_4Mg_3Ga_9N$.

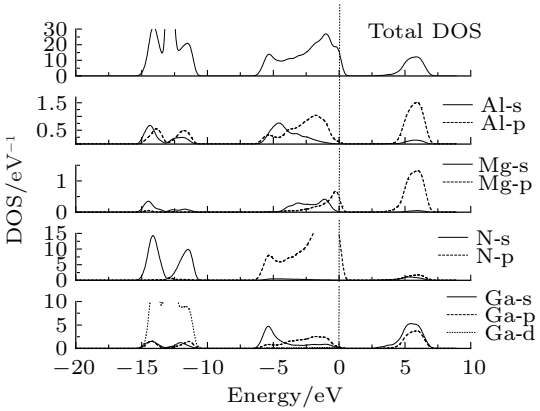


Fig. 4. Partial and total DOSs of $Al_4Mg_3Ga_9N$.

Figure 5 shows the charge differential densities of the (0001) direction before (Fig. 5(a)) and after (Fig. 5(b)) optimum Mg–Al co-doping. After doping, the properties of the bonds between the atoms change, the interactions between the atoms are different, and the charges are redistributed. The electron cloud of the N atoms is uniformly distributed in three directions, joining Ga atoms in the plane parallel to the *c* axis as shown in Fig. 5(a). The overlap population and the bond length of pure GaN in the direction parallel to the *c* axis are different from those in the direction vertical to the *c* axis (Table 3), which indicates that the covalent bonds between Ga and N atoms are directional and contain ionic bond characteristics.

For co-doped GaN, there is a large change in charge distribution around the doping atoms. The distribution characteristics of the charge between the doping atoms and its adjacent atoms can be seen in Fig. 5(b). When Mg atoms replace Ga atoms, the electrons of the adjacent N atoms move towards Ga atoms and away from the Mg atoms, the overlap population becomes negative, and the bond length increases between the Mg and N atoms (Table 3). This is because the electronegativity of Mg is lower than that of N, and Mg and its adjacent N atoms form strong ionic bonds. When Al atoms replace Ga atoms, the electrons of the adjacent N atoms move towards the Al atoms, the overlap population between the Al and N atoms increases, and the covalent bond of Al–N is stronger than that of Ga–N. In addition, Al doping makes the interaction between Ga and N weaker, thus the overlap population decreases, the bond length increases, the Ga 4s states move to a high energy, and the system band gap widens. The directivity of the band is enhanced after Mg–Al co-doping.

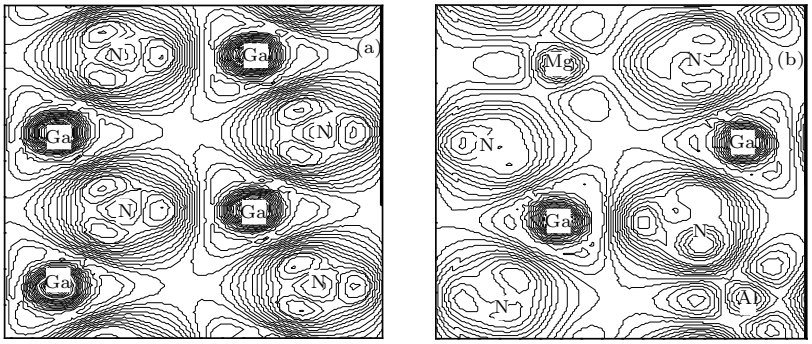


Fig. 5. Electron density differences in the (0001) plane (a) before and (b) after doping.

Table 3. Overlap populations and bond lengths.

System	Undoped		Co-doped					
Bond	N–Ga vertical to c axis	N–Ga parallel to c axis	N–Ga vertical to c axis	N–Ga parallel to c axis	N–Mg vertical to c axis	N–Mg parallel to c axis	N–Al vertical to c axis	N–Al parallel to c axis
Overlap population	0.66	0.58	0.60	0.59	–0.69	–0.71	0.67	0.67
Bond length /nm	0.1979	0.1971	0.1963	0.2015	0.2076	0.2068	0.1891	0.1898

5. Optical properties of the co-doped system

We also calculate the complex dielectric function, reflective index, refractive index, and extinction coefficient of GaN after optimum Mg–Al co-doping. The band gap of GaN is calculated to be 1.66 eV, which is smaller than an experimental value of 3.39 eV. The underestimation of the calculated band gap is a problem of the local density approximation (LDA) and GGA; however, this does not affect the results of the theoretical analysis. A scissor-operator correction of 1.73 eV is adopted in the co-doped system. The optimum Mg–Al co-doped GaN system is a direct band gap semiconductor. Its spectra are generated by electronic transitions between energy levels, and its dielectric function peaks can be explained by the band structure and the DOS. Figure 6 shows the real part (ε_1) and imaginary part (ε_2) of the dielectric function changing with incident photon energy (E). Figure 6(a) shows the case where E is vertical to z axis in the xy plane, and figure 6(b) displays the case where E is parallel to z axis. The static dielectric constant is calculated to be $\varepsilon_{1xy}(0) = 18.97$. In the low energy region, ε_{1xy} increases with photon energy increasing, and rapidly decreases in the energy region 1.20 eV–2.70 eV, corresponding to the reflection peak at 3.85 eV. The two peaks of the imaginary part ε_{2xy}, corresponding to the photon energies of 1.93 eV and 8.22 eV, indicates that there appears light absorption in the energy region compared with the case of the undoped system. The peak corresponding to the photon energy of 1.93 eV is generated by the interaction between Al 3p and N 2ps states, while the peak at 8.22 eV is generated by the interaction between Al 3p and Ga 3d states. In the direction parallel to the z axis, $\varepsilon_{1Z}(0) = 15.79$. The dielectric function in the xy plane and the dielectric function in the direction parallel to the z axis have the same locations of peaks. However, the sizes of the peaks are different in the low energy region, although they are identical when the photon energy is greater than 4.26 eV. Thus, the co-doped system shows anisotropy in the 0 eV–4.26 eV energy range.

Figure 7 shows the refractive index $n(\omega)$ and extinction coefficient $k(\omega)$ of the co-doped system. The static refractive index $n_0 = 4.35$, is bigger than that of undoped system(1.75 eV),[10] $n(\omega)$ has its peak and valley on the rising and falling edges of $k(\omega)$, $k(\omega)$ has its peak and valley at the maximum gradients of ε_1 (ω) rising and ε_2 (ω) falling, respectively, and the corresponding photon energies are 2.10 eV, 4.84 eV, 8.46 eV, and 14.99 eV. In the low energy region 2.10 eV–4.84 eV and the high energy region 8.46 eV–14.99 eV, $\varepsilon_{1xy}(\omega) < 0$, $k(\omega) > n(\omega)$, and the reflection coefficients (Fig. 8) are 0.80 eV, 0.87 eV, at 3.85 eV, and 14.51 eV, respectively, greater than those of the undoped system. The

absorption coefficient (Fig. 9) has a minimum less than that of the undoped system, and co-doped GaN shows metal reflective properties.

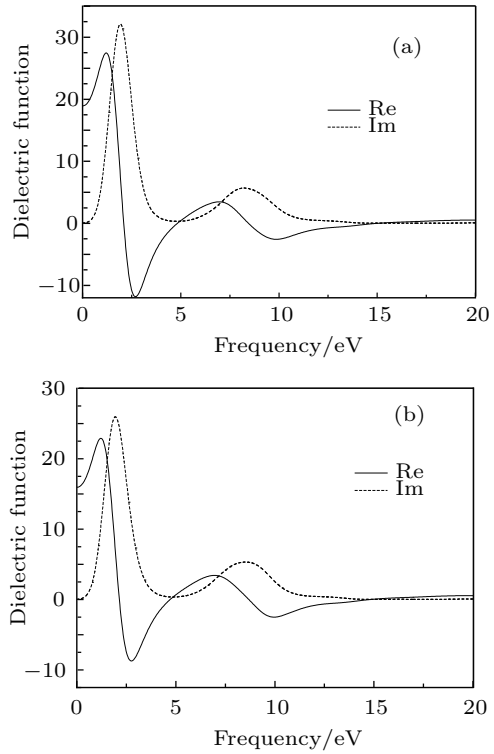


Fig. 6. Dielectric functions in the cases where (a) E is vertical to z axis and (b) E is parallel to z axis.

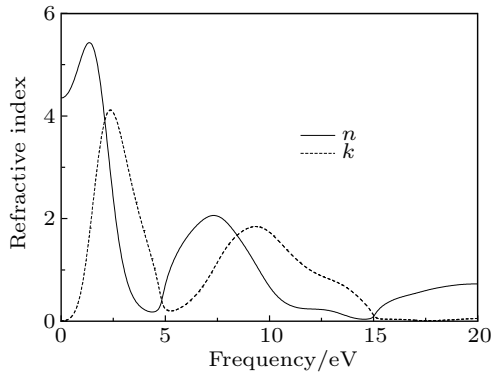


Fig. 7. Refractive indexes versus frequency of $Al_4Mg_3Ga_9N$.

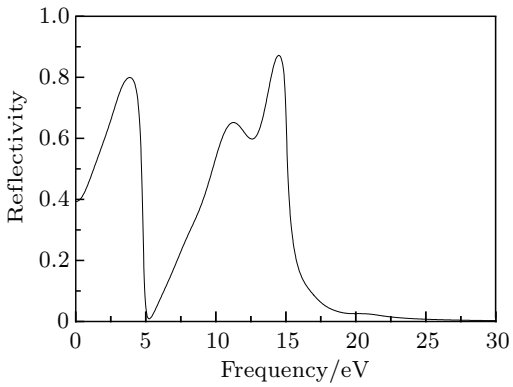


Fig. 8. Reflectivity versus frequency of $Al_4Mg_3Ga_9N$.

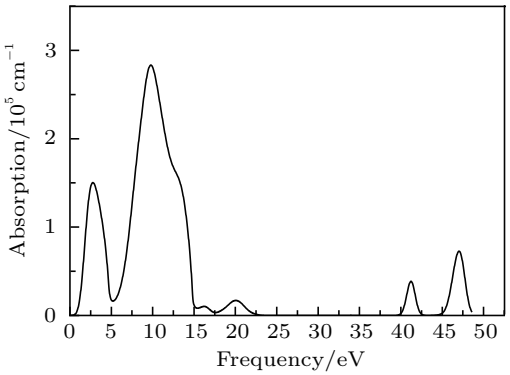


Fig. 9. Absorption versus frequency of $Al_4Mg_3Ga_9N$.

6. Conclusions

The electronic structure and optical properties of Al–Mg co-doped GaN are calculated using density functional theory. The results show that an appropriate concentration and ratio of Al and Mg can give an optimal co-doped system. The mutual exclusion function between acceptors produced by Mg doping can be overcome and the acceptor level can be reduced by controlling the concentration of Al. After optimum co-doping, the bonds between the atoms and the optical properties are anisotropic, the band gap widens, the refractive index increases, the absorption coefficient decreases, and the metal reflection characteristics are enhanced. Thus, a p-type semiconductor with a wide band gap, large refractive index, and a small absorption coefficient can be obtained by doping GaN with an appropriate concentration and ratio of Al and Mg.

References

[1] Zhao H P, Liu G Y and Tansu N 2010 *Appl. Phys. Lett.* **97** 131114
[2] Chow W W 2011 *Opt. Express* **19** 21818
[3] Farrell R M, Hsu P S, Haeger D A, Fujito K, DenBaars S P, Speck J S and Nakamura S 2010 *Appl. Phys. Lett.* **96** 231113
[4] Zhang J, Zhao H P and Tansu N 2011 *Appl. Phys. Lett.* **98** 171111
[5] Wang X H, Chang B K, Du Y J and Qiao J L 2011 *Appl. Phys. Lett.* **99** 042102
[6] Wang X H, Chang B K, Ren L and Gao P 2011 *Appl. Phys. Lett.* **98** 082109
[7] Li Y H, Pan H H and Xu P S 2005 *Acta Phys. Sin.* **54** 317 (in Chinese)
[8] Bar-Ilan A H, Zamir S, Katz O, Meyler B and Salzman J 2001 *Mater. Sci. Eng. A* **302** 14
[9] Zhang X F, Wang L, Liu J, Wei L and Xu J 2013 *Chin. Phys. B* **22** 017202
[10] Du Y J, Chang B K, Fu X Q, Wang X H and Wang M S 2012 *Optik* **123** 2208
[11] Akasaki I, Amano H, Koide Y, Hiramatsu K and Sawaki N 1989 *J. Cryst. Growth* **98** 209
[12] Vennéguès P, Leroux M, Dalmasso S, Benaissa M, Mierry P D, Lorenzini P, Damilano B, Beaumont B, Massies J and Gibart P 2003 *Phys. Rev. B* **68** 235214
[13] Takeshi I, Shigeru Y, Yoshifumi I and Teruaki M 2005 *J. Cryst. Growth* **274** 1
[14] Glaser E R, Murthy M, Freitas J A, Storm D F, Zhou L and Smith D J 2007 *Physica B* **401** 327
[15] Pezzagna S, Vennéguès P, Grandjean N and Massies J 2004 *J. Cryst. Growth* **269** 249
[16] Du Y J, Chang B K, Zhang J J, Wang X H, Li B and Wang M S 2011 *Optoelectron. Adv. Mat.* **5** 1050

[17] As D J, Frey T and Bartels M 2001 *J. Cryst. Growth* **230** 421
[18] Jang S H, Lee S S, Lee O Y and Lee C R 2003 *J. Cryst. Growth* **255** 220
[19] Li Z Y 2010 *The Electronic Structure and Optical Properties of Doped GaN* (M.S. Thesis) (Qufu: Qufu Normal University) (in Chinese)
[20] Lee S N, Son J K, Sakong T, Lee W, Paek H, Yoon E, Kim J, Cho Y H, Nam O and Park Y 2004 *J. Cryst. Growth* **272** 455
[21] Lei T, Moustakas T D, Graham R J, He Y and Berkowitz S J 1992 *J. Appl. Phys.* **71** 4933
[22] Perdew P, Burke K and Ernzerhof M 1996 *Phys. Rev. Lett.* **77** 3865
[23] Laasonen K, Pasquarello A, Car R, Lee C and Vanderbilt D 1993 *Phys. Rev. B* **47** 10142
[24] Monkhorst H J and Pack J D 1976 *Phys. Rev. B* **13** 5188
[25] Rosa A L and Neugebauer J 2006 *Phys. Rev. B* **73** 205346
[26] Xing H Y, Fan G H, Zhou T M and Li S T 2008 *Acta Phys.-Chim. Sin.* **24** 1432 (in Chinese)
[27] Xing H Y, Fan G H, Zhang Y and Zhao D G 2009 *Acta Phys. Sin.* **58** 450 (in Chinese)
[28] Cheng B W, Yao F, Xue C L, Zhang J G, Li Cb, Mao R W, Zuo Y H, Luo L P and Wang Q M 2005 *J. Semicond.* **26** 39 (in Chinese)
[29] Tetsuya Y and Hiroshi K Y 1998 *J. Cryst. Growth* **189** 532
[30] Gao C X, Yu F C, Choi A R, Kim D J, Kim C G, Kim C S, Kim H J and Ihm Y E 2006 *J. Cryst. Growth* **291** 60
[31] Bhattacharyya A, Moustakas T D, Zhou L, Smith D J and Hug W 2009 *Appl. Phys. Lett.* **94** 181907
[32] Liu N Y, Liu L, Wang L, Yang W, Li D, Li L, Cao W Y, Lu C M, Wan C H, Chen W H and Hu X D 2012 *Chin. Phys. B* **21** 117304